

# Tailoring Atropisomeric Maleimides for Stereospecific [2 + 2] Photocycloaddition—Photochemical and Photophysical Investigations Leading to Visible-Light Photocatalysis

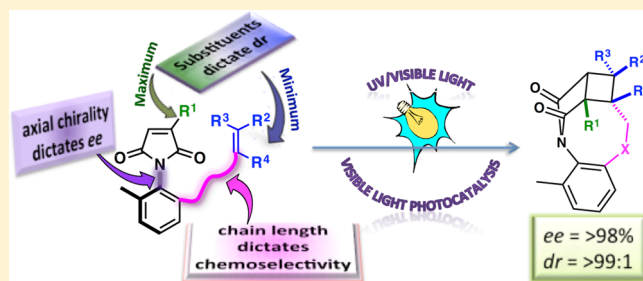
Elango Kumarasamy,<sup>†,§</sup> Ramya Raghunathan,<sup>†,§</sup> Steffen Jockusch,<sup>‡</sup> Angel Ugrinov,<sup>†</sup> and J. Sivaguru<sup>\*,†</sup>

<sup>†</sup>Department of Chemistry and Biochemistry, North Dakota State University, Fargo, North Dakota 58108, United States

<sup>‡</sup>Department of Chemistry, Columbia University, New York, New York 10027, United States

**S** Supporting Information

**ABSTRACT:** Atropisomeric maleimides were synthesized and employed for stereospecific [2 + 2] photocycloaddition. Efficient reaction was observed under direct irradiation, triplet-sensitized UV irradiation, and non-metal catalyzed visible-light irradiation, leading to two regioisomeric (*exo/endo*) photoproducts with complete chemoselectivity (exclusive [2 + 2] photoproduct). High enantioselectivity (*ee* > 98%) and diastereoselectivity (*dr* > 99:1%) were observed under the employed reaction conditions and were largely dependent on the substituent on the maleimide double bond but minimally affected by the substituents on the alkenyl tether. On the basis of detailed photophysical studies, the triplet energies of the maleimides were estimated. The triplet lifetimes appeared to be relatively short at room temperature as a result of fast [2 + 2] photocycloaddition. For the visible-light mediated reaction, triplet energy transfer occurred with a rate constant close to the diffusion-limited value. The mechanism was established by generation of singlet oxygen from the excited maleimides. The high selectivity in the photoproduct upon reaction from the triplet excited state was rationalized on the basis of conformational factors as well as the type of diradical intermediate that was preferred during the photoreaction.

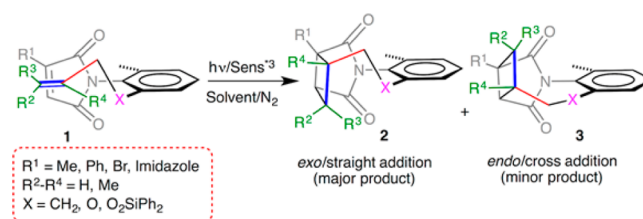


## INTRODUCTION

The importance of synthesizing optically pure molecules has placed asymmetric organic synthesis among the most explored areas in chemistry.<sup>1</sup> However, the absence of a single universal method to access desired chiral scaffold(s) has forced chemists to develop strategies that are both elegant and effective. In the gamut of methodologies developed in organic synthesis, asymmetric photochemical transformations<sup>2</sup> hold a unique place as they can provide access to molecules with unique stereochemical and structural complexity, thus serving as a complementary avenue to thermal transformations.<sup>3</sup> Photoreactions are inherently fast processes that present challenges to manipulate the excited-state reactivity and product stereochemistry in the desired reaction. Recent advances such as photoreactions in confined media, photoreactions controlled by supramolecular templates, and solid-state photoreactions have addressed this bottleneck to some extent and have led to improvements in the control of product selectivity.<sup>4</sup> In spite of the improvement obtained by employing organized assemblies, achieving stereoselectivity in photoreactions that occur in solution has presented formidable challenges. In that regard, we have embraced a strategy that employs atropisomeric compounds,<sup>5</sup> where axial chirality in the reactant is transferred to point chirality in the product upon excitation in the desired photochemical transformation.<sup>6</sup> We

have successfully demonstrated the efficacy of this strategy in various photochemical transformations,<sup>6</sup> including  $6\pi$  photocyclization,<sup>6a,b</sup>  $4\pi$  photocyclization,<sup>6c,d</sup> [2 + 2] photocycloaddition,<sup>6e</sup> Norrish–Yang cyclization,<sup>6f,g</sup> and Paternò–Büchi reactions.<sup>6h</sup> To broaden the scope of this strategy to access chirally enriched photoproducts, we looked at [2 + 2] photocycloaddition of atropisomeric maleimides. In this report, we disclose our results on the stereospecific [2 + 2] photocycloaddition of atropisomeric maleimides (Scheme 1) that can be performed by visible-light mediated energy transfer, in which we were able to achieve high enantio-

### Scheme 1. Intramolecular [2 + 2] Photocycloaddition of Atropisomeric Maleimides 1



Received: April 7, 2014

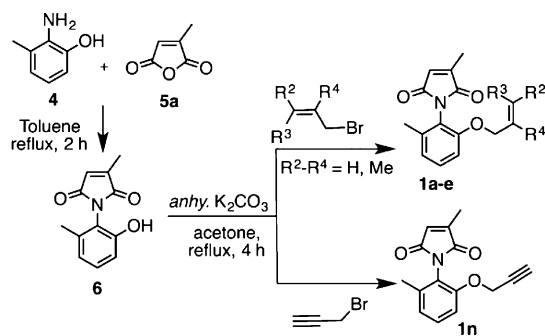
lectivity ( $ee > 98\%$ ), diastereoselectivity (*exo/endo* selectivity), and chemoselectivity ( $[2 + 2]$  vs  $[5 + 2]$  cycloaddition) in the product by appropriate substitution on the atropisomeric maleimides.

Maleimides display rich and versatile chemistry in both the ground state (thermal reactions) and the excited state (photochemical reactions).  $[2 + 2]$ ,  $[4 + 2]$ , and  $[5 + 2]$  cycloadditions are a few of the reactions that are initiated by photons.<sup>7</sup> Depending on the substrate, type of irradiation (sensitized vs direct irradiation), and wavelength, one can switch from one product to another.<sup>7c,8</sup> Booker-Milburn and others have extensively investigated  $[2 + 2]$  and  $[5 + 2]$  photocycloadditions of maleimides to access certain complex organic scaffolds with multiple stereogenic centers.<sup>7c,9</sup> They have also elegantly demonstrated the possibility of large-scale synthesis by merging photoreactions with a flow setup and extending this technique to natural product synthesis.<sup>10</sup> However, stereoselective photoreactions of maleimides have been only scarcely investigated. We felt that incorporating our methodology of axial-to-point chiral transfer in maleimides would enable us to perform stereospecific photocycloaddition reactions and further increase the scope and versatility of the maleimides.

## RESULTS AND DISCUSSION

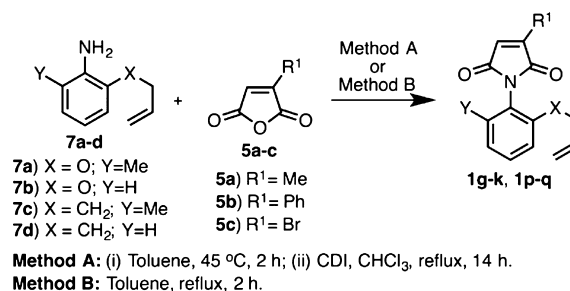
Atropisomeric maleimides<sup>11</sup> with varying substitution patterns were synthesized to evaluate how substituent(s) on (a) the maleimide ring ( $R^1 = \text{alkyl, aryl, halogen}$ ), (b) the *N*-aryl ring ( $X = \text{CH}_2, \text{O}, \text{O}_2\text{SiPh}_2$ ), and (c) the alkenyl tether ( $R^2, R^3, R^4 = \text{H or alkyl}$ ) influence the  $[2 + 2]$  photocycloaddition. Most of the maleimides were synthesized using one of the two methods shown in Schemes 2 and 3. For example, maleimides **1a–e** and **1n** ( $R^1 = \text{Me}$ ) were easily obtained by the reaction of 2-amino-3-methylphenol (**4**) with citraconic anhydride (**5a**) followed by allylation in the presence of a base (Scheme 2). However,

### Scheme 2. Synthesis of Maleimides **1a–e** and **1n**



maleimide derivatives **1g–k**, **1p**, and **1q** with bromo or phenyl substituents ( $R^1 = \text{Ph, Br}$ ) underwent decomposition by this approach, so these compounds were accessed starting from allylated aniline derivatives **7a–d** (Scheme 3). The yields of these methods were generally good for two-step reactions.<sup>12</sup> The atropisomeric maleimides were then characterized by <sup>1</sup>H and <sup>13</sup>C NMR spectroscopy, high-resolution mass spectrometry (HRMS), circular dichroism, and specific rotation values.<sup>12</sup> The optically pure isomers of the atropisomeric maleimides for the study were easily secured through preparative separations on a chiral stationary phase using HPLC and usually had  $>98\%$  enantiomeric purity.<sup>12</sup>

### Scheme 3. Synthesis of Maleimides **1g–k**, **1p**, and **1q**



One of the characteristic features of atropisomeric compounds (compounds whose chirality originates from restricted rotation around a single bond) is their tendency to racemize at elevated temperature. Such racemization erodes the absolute configuration, resulting in poor selectivity in the desired stereospecific transformations. On the basis of computational analysis, it was reasoned that *N*-phenylmaleimides prefer a twisted orientation with respect to the *N*–C(aryl) axis to avoid steric crowding between the imide carbonyls and the ortho hydrogens of the aryl group.<sup>13</sup> Additionally, suitable substitutions at the ortho positions (i.e., the 2- and 6-positions) of the *N*-phenyl ring should result in atropisomeric maleimides with a stable chiral axis that would enable us to transfer/trap the axial chirality in the reactant to point chirality in the photoproduct.<sup>11,14</sup> In this regard, the methyl group at the 6-position of the *N*-phenyl ring in newly synthesized maleimides **1** was crucial in providing stable atropisomers by increasing the energy barrier for the *N*–C(aryl) bond rotation. Maleimides lacking the Me group at the 6-position (analogues of maleimides **1a**, **1g**, and **1j**) were not axially chiral at room temperature.<sup>14a</sup> Analysis of the kinetic parameters for the newly synthesized atropisomeric maleimides **1a–c** and **1g** provided insights into the energy barrier to rotation around the *N*–C(aryl) chiral axis (Table 1). For example, in the case of **1a**

**Table 1. Racemization Kinetics of Optically Pure Atropisomeric Maleimides **1** in Toluene at 100 °C<sup>a</sup>**

**1a:** R<sup>1</sup>=Me; R<sup>2</sup>,R<sup>3</sup>=H  
**1b:** R<sup>1</sup>,R<sup>2</sup>,R<sup>3</sup>=Me  
**1c:** R<sup>1</sup>,R<sup>2</sup>=Me;R<sup>3</sup>=H  
**1g:** R<sup>1</sup>=Ph; R<sup>2</sup>,R<sup>3</sup>=H

entry	compd	$k_{\text{rac}}$ (s <sup>-1</sup> )	$\tau_{1/2}$ (days)	$\Delta G_{\text{rac}}^\ddagger$ (kcal mol <sup>-1</sup> )
1	<b>1a</b>	$2.27 \times 10^{-6}$	3.5	31.6
2	<b>1b</b>	$2.22 \times 10^{-6}$	3.6	31.7
3	<b>1c</b>	$2.33 \times 10^{-6}$	3.5	31.6
4	<b>1g</b>	$2.40 \times 10^{-6}$	3.4	31.6

<sup>a</sup>The racemization kinetics was followed by HPLC analysis on a chiral stationary phase. Values carry an error of  $\pm 5\%$ .<sup>12</sup>

(Table 1, entry 1), the half-life for racemization ( $\tau_{1/2}$ ) was 3.5 days at 100 °C, corresponding to a racemization rate constant ( $k_{\text{rac}}$ ) of  $2.27 \times 10^{-6} \text{ s}^{-1}$  and an activation energy barrier ( $\Delta G_{\text{rac}}^\ddagger$ ) of  $\sim 31.6 \text{ kcal mol}^{-1}$ . The racemization energy barrier was not affected significantly by variation of the  $R^1$  substituent on the maleimide double bond or the substituent on the alkenyl tether with **1a–c** and **1g** (Table 1; entries 1–4) having similar energy barriers for racemization. Inspection of Table 1 suggests that the newly synthesized atropisomeric maleimides have fairly high energy barriers and can be employed effectively for

photoreactions at ambient temperature without the loss of absolute configuration.

The [2 + 2] photocycloadditions of the atropisomeric maleimides were carried out under different irradiation conditions and proceeded smoothly in excellent isolated yields and mass balance (Tables 2–4). Three different sets of irradiation conditions were examined: (a) direct irradiation; (b) sensitized irradiation under UV light (e.g., using xanthone as a sensitizer); and (c) sensitization under metal-free visible-light irradiation (e.g., using thioxanthone as a sensitizer). After the photoreaction, the solvent was removed under reduced pressure, and the product(s) were purified by column chromatography. The HPLC, NMR, and X-ray diffraction (XRD) analyses revealed that the major photoproduct was the *exo*-photoadduct **2** (where *exo* indicates that the terminal carbon of the alkene tether is oriented away from the carbon bearing the R<sup>1</sup> substituent of the maleimide) and the minor photoproduct was *endo*-photoadduct **3** (where *endo* indicates that the terminal carbon of the alkene tether is oriented toward the carbon bearing the R<sup>1</sup> substituent of the maleimide). We employed **1a** as a model system to optimize the irradiation conditions (Tables 2 and 3). Direct irradiation of **1a** in acetonitrile gave a 2:3 diastereomeric ratio (dr) of 79:21 (Table 2, entries 1–3). The dr was unaffected but the conversion was

**Table 2. Direct and Sensitized Irradiation of 1a<sup>a</sup>**

entry	irradiation conditions	solvent	2:3 (% conv.)
1	bb/Pyrex cutoff, 12 h	MeCN	79:21 (>98)
2	~300 nm, N <sub>2</sub> , 6 h	MeCN	79:21 (93)
3	~300 nm, O <sub>2</sub> , 6 h	MeCN	79:21 (88)
4	~300 nm, -30 °C, 12 h	MeCN	79:21 (31)
5	bb/Pyrex cutoff, N <sub>2</sub> , 1.5 h	acetone <sup>b</sup>	79:21 (84 <sup>c</sup> )
6	~350 nm, xanthone, 1 h	MeCN	79:21 (>98)
7	~420 nm, thioxanthone, 1 h	MeCN	79:21 (>98)

<sup>a</sup>Irradiation was performed at room temperature, unless otherwise noted. Values are based on <sup>1</sup>H NMR spectroscopy (±5% error). [**1a**] ≈ 3.9 mM. bb/Pyrex cutoff = broadband irradiation performed using a 450 W mercury lamp with a Pyrex cutoff filter (<295 nm cutoff); ~300 nm, ~350 nm, and ~420 nm irradiations were carried out in a Rayonet reactor. <sup>b</sup>Acetone was used as the solvent and sensitizer. <sup>c</sup>Isolated yield.

affected by a decrease in temperature (Table 2, entry 4). In addition, the efficiency of the reaction and the dr were similar under oxygen- and nitrogen-saturated atmospheres (Table 2; compare entries 2 and 3). When the solvent was changed to acetone, which acted both as a solvent and a triplet sensitizer, the reaction efficiency was significantly improved, and the reaction required a shorter irradiation time (Table 2, entry 5) and afforded an excellent isolated yield of the photoproducts. The reaction was equally efficient when the triplet sensitizer was changed to xanthone (~350 nm irradiation) or thioxanthone (~420 nm irradiation). There was no change in the dr when the irradiation conditions were changed from direct irradiation to triplet sensitization. To study the effect of solvent on the reaction, we employed different solvents for xanthone and thioxanthone sensitization (Table 3). Excellent mass balance and very high to moderate conversions were observed for all of the solvents except tetrahydrofuran (THF), in which decomposition was observed. The conversion was slightly lower in benzene and in methylcyclohexane (MCH).

**Table 3. Solvent Screening Studies under Triplet-Sensitized Irradiation of 1a<sup>a</sup>**

entry	solvent	% conversion (% mass balance)	
		xanthone	thioxanthone
1	methanol	>98 (>98)	>98 (>98)
2	MeCN	>98 (>98)	>98 (>98)
3	ethyl acetate	>98 (95)	83 (>98)
4	THF	– <sup>b</sup>	–
5	chloroform	>98 (81)	>98 (>98)
6	CH <sub>2</sub> Cl <sub>2</sub>	>98 (>98)	>98 (>98)
7	benzene	44 (78)	73 (>98)
8	MCH	27 (>98)	26 (>98)

<sup>a</sup>[**1a**] ≈ 3.9 mM; wavelengths of ~350 and ~420 nm were used for xanthone- and thioxanthone-sensitized irradiation in a Rayonet reactor at room temperature. Conversion and mass balance were determined by <sup>1</sup>H NMR spectroscopy using triphenylmethane as an internal standard (±5% error). <sup>b</sup>The product decomposed after sensitized irradiation with xanthone.

The irradiation conditions for maleimides **1a–n** were carefully chosen after several optimization studies to obtain the best results.<sup>12</sup> For example, irradiation in acetone was very efficient for all of the maleimides except **1g**, **1j**, and **1m**, which partially decomposed,<sup>15</sup> resulting in significantly lower isolated yields. To overcome this decomposition, we employed xanthone and thioxanthone as sensitizers in MeCN, which resulted in very high isolated yields. This set of conditions also worked with equal efficiency for other maleimides as well, enabling us to develop visible-light mediated photocatalytic conditions for our transformations. The reaction optimization was done to minimize the established [5 + 2] photocycloaddition that typically competes with the [2 + 2] dimerization reaction.<sup>16</sup> Under our reaction conditions (direct or triplet-sensitized irradiation), we did not observe photoproducts corresponding to [5 + 2] cycloaddition. We believe that the observed chemoselectivity ([5 + 2] vs [2 + 2]) was a reflection of the molecular constraints that enforced reactivity between the maleimide double bond and the alkenyl tether. The reaction efficiency/conversion was higher under triplet sensitization, as the reaction proceeded to complete conversion in 1–2 h while 8–12 h was required for direct irradiation, with no appreciable change in the observed selectivities (ee and dr values) in the photoproduct.

Investigation of Table 4 reveals several interesting features of the [2 + 2] photocycloaddition reaction of atropisomeric maleimides. The enantioselectivities of all the atropisomeric maleimides investigated were >98% (Table 4, **1a–d** and **1g**). This was due to the high energy barrier to rotation around the N–C(aryl) chiral axis (Table 1), which prevented racemization during the photoreaction and enabled efficient axial-to-point chirality transfer, leading to excellent enantiomeric excess in the photoproduct(s). Satisfied with the excellent enantiocontrol in the [2 + 2] photocycloaddition reaction, we screened several atropisomeric maleimides to analyze the *exo/endo* ratio (i.e., the dr) in the resulting photoproducts. To understand the origin of the diastereoselectivity between **2** and **3**, we systematically varied the R<sup>1</sup> substituent on the maleimide double bond, the R<sup>2</sup>–R<sup>4</sup> substituents on the alkenyl tether, and the X group that links the alkenyl tether to the N-aryl ring. The X group had very little influence over the dr (Table 4; compare **1a** with **1i** and **1h** with **1k**). Even a longer alkenyl tether as in the case of **1f** did not result in better dr (Table 4, entry 6). This was a slight

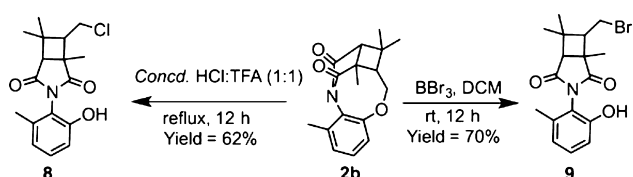
Table 4. Intramolecular [2 + 2] Photocycloaddition of Atropisomeric Maleimides<sup>a,b</sup>

Entry	Substrate	Major photoproduct	Isolated yield dr (2:3), <sup>c</sup> % ee	Entry	Substrate	Major photoproduct	Isolated yield [%] dr (2:3), <sup>c</sup> % ee
1			84 (79:21) > 98% ee > 98% ee	8			82 (69:31)
2			60 (79:21) > 98% ee > 98% ee	9			88 (74:26)
3			84 (87:13) > 98% ee > 98% ee	10			82 (> 99:1)
4			90 <sup>e</sup> (84:16) > 98% ee > 98% ee	11			80 (61:39)
5			77 (62:38)	12			94 (42:58)
6			76 (77:23)	13			74 (>99:1)
7			90 (> 99:1) > 98% ee > 98% ee	14		Dimers / Decomposition	

<sup>a</sup>Irradiation of **1b** was performed with 30 mol % xanthone as the triplet sensitizer in acetonitrile solvent at room temperature using a Rayonet reactor equipped with 300 nm lamps. Irradiations of **1g**, **1j**, and **1m** were performed with 30 mol % thioxanthone as the triplet sensitizer in acetonitrile solvent at room temperature using a Rayonet reactor equipped with 420 nm lamps. For all other substrates, the photoreactions were performed in acetone at room temperature using a 450 W medium-pressure Hg lamp with a Pyrex cutoff filter. <sup>b</sup>The ee values were obtained from HPLC analysis on a chiral stationary phase, and the results are averages of three runs with an error of  $\pm 3\%$ . The absolute configuration was determined by XRD with Flack parameters. <sup>c</sup>The ratios were determined by <sup>1</sup>H NMR spectroscopy of the crude samples. <sup>d</sup>A and B refer to the order of HPLC elution for a given pair of enantiomers. <sup>e</sup>Yield based on <sup>1</sup>H NMR spectroscopy using triphenylmethane as an internal standard.

disappointment in our case, as the silyl tether was established to have control over the diastereoselectivity during photocycloaddition.<sup>17</sup> However, to our delight, when phenyl derivatives **1g** (X = O) and **1j** (X = CH<sub>2</sub>) and imidazole derivative **1m** were subjected to [2 + 2] photocycloaddition, complete control of the dr was observed, and the *exo* photocycloadduct **2** was obtained as the sole product (Table 4, entries 7, 10, and 13). In the case of **1g** (Table 4, entry 7), in addition to the excellent diastereomeric ratio (dr > 99:1), excellent enantiomeric excess (ee > 98%) and isolated yield (90%) of the *exo* photoproduct **2** were observed during the [2 + 2] photocycloaddition. These results allowed us to believe that the substituent at the maleimide double bond (the R<sup>1</sup> substituent) plays a more significant role in controlling the dr in the photoproducts than the X group in the alkenyl tether. For example, in the reactions of **1a**, **1g**, **1h**, and **1m** with varying R<sup>1</sup> substitution (Table 4, entries 1, 7, 8, and 13), the dr varied significantly: 69:31 for substrate **1h** with R<sup>1</sup> = Br (entry 8); 79:21 for substrate **1a** with R<sup>1</sup> = Me (entry 1); and >99:1 for substrates **1g** and **1m** with phenyl and imidazole substituents, respectively (entries 7 and 13). Surprisingly, disubstitution at the maleimide double bond as in **11** gave a dr of 42:58 favoring the *endo* product **31** in 94% isolated yield (Table 4, entry 12). Having ascertained the role of the R<sup>1</sup> and X substituents during intramolecular [2 + 2] photocycloaddition in maleimides, we then turned our attention to substituents on the alkene portion of the tether (R<sup>2</sup>–R<sup>4</sup>) to understand the scope and limitations of our substrates. We designed four different substrates **1b–e** and compared the dr values to gain insights into the role of the alkene geometry during the [2 + 2] photocycloaddition. Comparison of the *exo/endo* ratios from the [2 + 2] photocycloaddition of **1a** and **1b** revealed that *gem*-dimethyl substitution at the terminal alkene carbon atom did not alter the dr value (2:3 = 79:21 in both cases; Table 4, entries 1 and 2). On the other hand, monomethyl substitution on the terminal carbon of the alkene resulted in a slight increase in the dr value from 79:21 for **1a** to 87:13 for **1c** and 84:16 for **1d** (Table 4; compare entries 1, 3 and 4). Internal substitution on the alkene double bond as in substrate **1e** resulted in a lower dr value (2:3 = 62:38) compared with **1a** (Table 4; compare entries 1 and 5). Interestingly, changing the reaction partner from alkene to alkyne in the case of maleimide **1n** did not yield the desired cyclobutene photoproducts,<sup>17</sup> although complete consumption of the starting material was observed. Careful analysis of the products by HRMS and <sup>1</sup>H NMR studies revealed that dimeric products were formed along with significant decomposition. Placement of oxygen on the alkenyl tether in the maleimide allowed us to cleave the tether after the photoreaction. The ether cleavage of the photoproducts proceeded smoothly with BBr<sub>3</sub> or 1:1 v/v concd. HCl/TFA (Scheme 4) to yield the corresponding *N*-arylphenols in isolated yields of 62–70%. However, to our disappointment the imide cleavage proved to be rather difficult under different conditions.<sup>12</sup>

#### Scheme 4. Cleavage of Photoproduct 2b



Detailed photophysical investigations were carried out in order to gain more insight into the excited state(s) of the maleimides and the mode of reactivity involving sensitized visible-light irradiation.<sup>13,18</sup> Fluorescence and phosphorescence measurements on maleimides were futile as the newly synthesized atropisomeric maleimides were poor luminophores. Even at 77 K the luminescence of the atropisomeric maleimides was negligible, indicating very fast decay of the excited state. Considering the reactivity of the maleimides, we designed maleimides **10** and **11** with a saturated alkenyl tether so that we could overcome the fast excited-state reactivity/deactivation and decipher the excited-state behavior/spin state involved using laser flash photolysis experiments (Figures 1–3).<sup>12</sup>

Laser excitation ( $\lambda_{\text{ex}} = 355$  nm, pulse width = 7 ns) of an argon-saturated solution of **10** in acetonitrile generated a transient absorption spectrum (Figure 1A, red). The transient

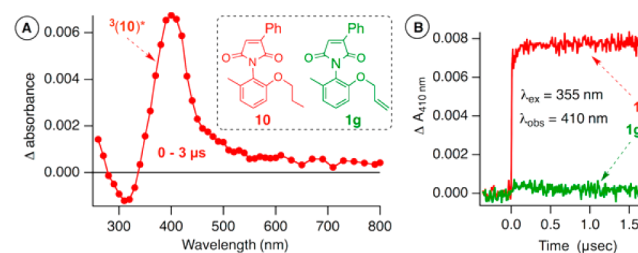


**Figure 1.** (A) Transient absorption spectrum monitored 0–3  $\mu\text{s}$  after pulsed laser excitation (355 nm, 7 ns pulse length) of an argon-saturated MeCN solution of **10**. (B) Absorbance kinetic traces (monitored at 410 nm) for argon-saturated MeCN solutions of **10** (red) and **1g** (green) with matching absorbance of 0.3 at 355 nm.

absorption centered around 400 nm decayed with a lifetime of 50  $\mu\text{s}$ , was quenched by molecular oxygen ( $k_{\text{q}} = 2 \times 10^9 \text{ M}^{-1} \text{ s}^{-1}$ ), and was assigned to the triplet–triplet absorption of the maleimide chromophore. The triplet transient of **10** was further confirmed by triplet energy transfer from excited thioxanthone (TX).

The initial triplet absorption of TX at 620 nm (Figure 2A, blue spectrum) was quenched by **10** to generate <sup>3</sup>**10**\* (Figure 2A, red spectrum) at later times. Having ascertained the triplet transient of maleimide **10**, we were able to investigate the triplet quantum yield by monitoring the efficiency of singlet oxygen generation in aerated CCl<sub>4</sub> solution (Figure 3). With phenalene as the reference ( $\Phi_{\Delta} = 0.98$ ),<sup>19</sup> the relative quantum yield for the generation of singlet oxygen from **10** upon pulsed laser irradiation was ascertained to be  $\Phi_{\Delta} \approx 0.04$ . This clearly established that the maleimides we investigated have a very poor intersystem crossing quantum yield and generate very low amounts of the triplet upon direct excitation.

Comparison of the triplet–triplet absorbance at 410 nm upon laser excitation at 355 nm for **10** (maleimide with a saturated alkyl tether) and **1g** (the corresponding maleimide with an alkenyl tether) under identical conditions showed only negligible amounts of detectable <sup>3</sup>**1g**\* compared with <sup>3</sup>**10**\* (Figure 1B). The absence of detectable <sup>3</sup>**1g**\* is likely due to the reactivity of the alkene double bond in **1g**, resulting in deactivation of the triplet state by the [2 + 2] photocycloaddition reaction. While maleimides reacted efficiently from the triplet excited state, as evidenced by the weak transient absorbance of **1g**, the generation of the triplet species by direct irradiation was inefficient, as ascertained by the low quantum yield of singlet oxygen generation from **10**, indicating

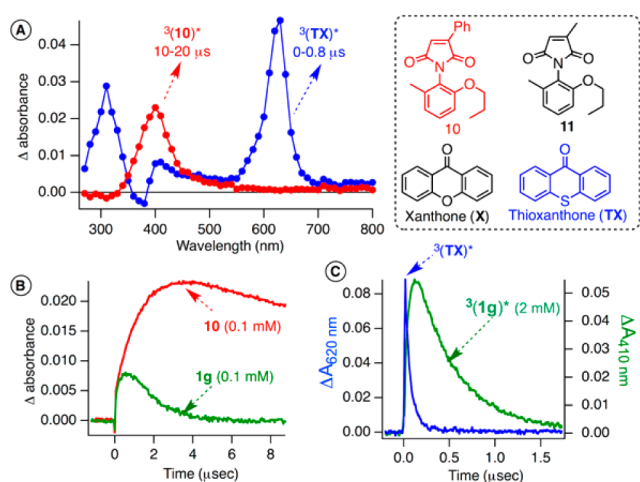


**Figure 2.** (A) Transient absorption spectra monitored at 0–0.8  $\mu\text{s}$  (blue) and 10–20  $\mu\text{s}$  (red) after pulsed laser excitation (355 nm, 7 ns pulse length) of argon-saturated MeCN solutions of TX and **10** (0.05 mM). (B) Absorbance kinetic traces (monitored at 410 nm) for argon-saturated MeCN solutions of TX containing 0.1 mM **10** (red) or **1g** (green). (C) Absorbance kinetic traces monitored at 620 nm (blue) and 410 nm (green) after pulsed laser excitation using the front-face geometry and a 2 mm optical path length.

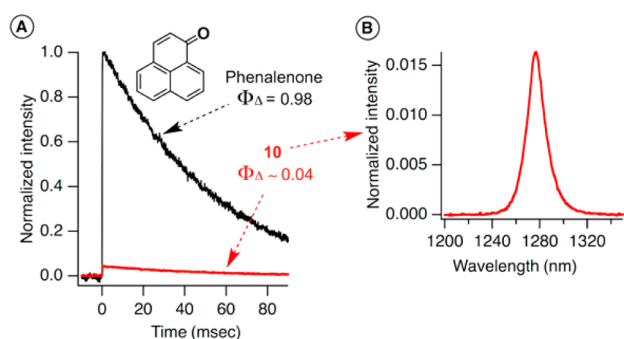


**Figure 3.** (A) Singlet oxygen phosphorescence decay traces (monitored at 1270 nm) generated by pulsed laser excitation (355 nm, 7 ns pulse length) of air-saturated  $\text{CCl}_4$  solutions of **10** (red) and phenalene (black) with matching absorbance of 0.3 at 355 nm. (B) Normalized singlet oxygen phosphorescence spectrum generated by steady-state irradiation of **10** at 355 nm in air-saturated  $\text{CCl}_4$  solution.

a very low efficiency of intersystem crossing from the singlet excited state to the triplet excited state of the maleimides (Figure 3). To improve the efficiency for generation of the triplet excited state, different sensitizers were employed to promote the chemical transformation. Considering the experimental aspects and the viability of using visible-light irradiation, we selected thioxanthone as the triplet sensitizer because its photophysical characteristics are well-established.

Laser excitation ( $\lambda_{\text{ex}} = 355 \text{ nm}$ ) of TX in the presence of maleimide **10** in argon-saturated acetonitrile solution gave the corresponding triplet species  ${}^310^*$ , as ascertained by the decay of the absorbance at 620 nm (corresponding to  ${}^3\text{TX}^*$ ) and the rise in the absorbance centered around 400 nm (corresponding to  ${}^310^*$ ) (Figure 2B, red). Similarly, laser excitation ( $\lambda_{\text{ex}} = 355 \text{ nm}$ ) of TX in the presence of **1g** (the parent maleimide with the alkenyl double bond) in argon-saturated acetonitrile solution produced the corresponding triplet transient  ${}^31g^*$ . In the presence of **1g**,  ${}^3\text{TX}^*$  acted as a triplet-excited-state donor and **1g** acted as an acceptor, as reflected in the decrease in the

absorbance intensity at 620 nm and the increase in the absorbance intensity centered around 410 nm (Figure 2B, green). This was again reflected in the absorbance kinetic profile monitored at 410 nm. On the basis of the decay of  ${}^31g^*$ , the triplet lifetime in argon-saturated acetonitrile was established to be 450 ns (Figure 2C) using laser excitation ( $\lambda_{\text{ex}} = 355 \text{ nm}$ ) of TX in a short optical path length of 2 mm with the front-face optical geometry.<sup>12</sup> Comparison of the triplet lifetimes of **1g** ( $\tau_T = 450 \text{ ns}$ ) and **10** ( $\tau_T = 50 \mu\text{s}$ ) showed that the alkenyl functionality in **1g** deactivated the excited triplet state of the maleimide, presumably by undergoing [2 + 2] photocycloaddition efficiently.

Bimolecular rate constants for quenching of the sensitizer's triplet states by maleimides ( $k_q$ ) were determined by laser flash photolysis (see the Supporting Information), and the results are summarized in Table 5. Inspection of Table 5 reveals that

**Table 5. Bimolecular Rate Constants for Quenching of Excited Triplet States of Sensitizers by Maleimides ( $k_q$ )<sup>a</sup>**

entry	triplet sensitizer	maleimide	$k_q$ ( $\text{M}^{-1} \text{s}^{-1}$ )
1	thioxanthone	<b>1a</b>	$(3.6 \pm 0.1) \times 10^9$
2	thioxanthone	<b>1i</b>	$(3.5 \pm 0.1) \times 10^9$
3	thioxanthone	<b>11</b>	$(3.5 \pm 0.1) \times 10^9$
4	xanthone	<b>11</b>	$(6.3 \pm 0.1) \times 10^9$
5	thioxanthone	<b>1g</b>	$(8.3 \pm 0.4) \times 10^9$
6	thioxanthone	<b>1j</b>	$(8.2 \pm 0.3) \times 10^9$
7	thioxanthone	<b>10</b>	$(7.9 \pm 0.4) \times 10^9$
8	xanthone	<b>10</b>	$(7.6 \pm 0.2) \times 10^9$

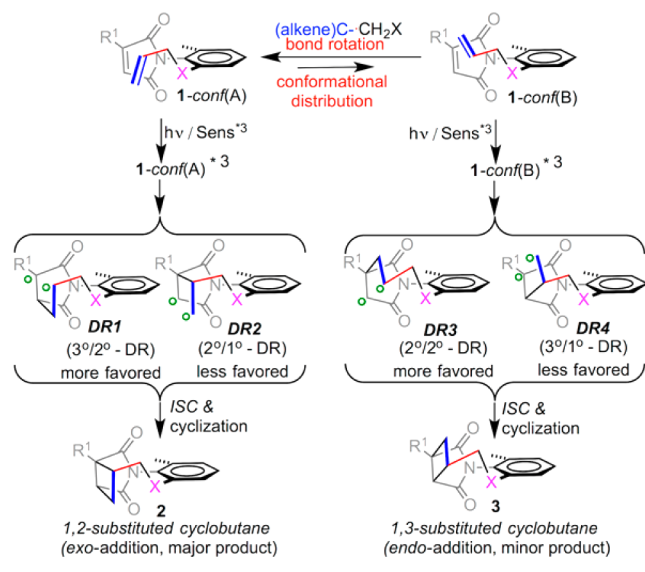
<sup>a</sup>Determined by laser excitation ( $\lambda_{\text{ex}} = 355 \text{ nm}$ ) of thioxanthone or xanthone (absorbance at 355 nm = 0.3) in the presence of varying concentrations of maleimides in argon-saturated MeCN. For details, see the Supporting Information.<sup>12</sup>

triplet excited states of xanthone and thioxanthone are efficiently quenched by maleimides with very high quenching rate constants that are close to the diffusion-limited values. The distinct quenching rate constants observed for maleimides **10** ( $R^1 = \text{Ph}$ ) and **11** ( $R^1 = \text{Me}$ ) toward xanthone and thioxanthone likely reflect the efficiencies of energy transfer from the excited sensitizers to the maleimides. For example, the triplet excited states of xanthone and thioxanthone were efficiently quenched by **10** with roughly the same rate constant (Table 5, entries 7 and 8). On the other hand, the rate constant for quenching of triplet-excited thioxanthone by **11** [ $k_q = (3.5 \pm 0.1) \times 10^9 \text{ M}^{-1} \text{ s}^{-1}$ ; Table 5, entry 3] was almost half of the rate constant for quenching of triplet-excited xanthone [ $k_q = (6.3 \pm 0.1) \times 10^9 \text{ M}^{-1} \text{ s}^{-1}$ ; Table 5, entry 4]. This decrease in the quenching rate constant reflects similar triplet energies for thioxanthone and methyl-substituted maleimides ( $\sim 63 \text{ kcal/mol}$ ). On the other hand, phenyl-substituted maleimides quenched the triplet states of both xanthone and thioxanthone efficiently because their triplet energies are likely well below the triplet energy of thioxanthone as a result of the extended conjugation of the maleimide chromophores with the phenyl ring.

On the basis of our photophysical investigations, we believe that the intramolecular [2 + 2] photocycloaddition of maleimides **1a–m** occurs via a triplet pathway. Mechanistically, the *exo/endo* photoproduct selectivity and the stereospecific chiral transfer need to be addressed. The electron-rich nature of the alkene tether likely triggers the photocyclization by the interaction with the half-filled  $\pi$  orbital of the  $\pi\pi^*$  excited state

of the maleimide.<sup>20</sup> We will first address the mechanistic aspects of triplet-sensitized reactions then discuss the mechanism of direct irradiation. We conjecture that the triplet-sensitized reaction (with UV or visible light) proceeds by a two-step process (Scheme 5) from the triplet excited state:

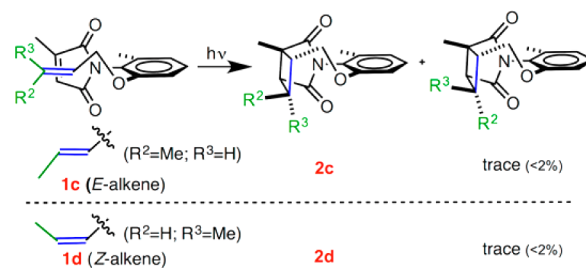
### Scheme 5. Mechanistic Rationale for [2 + 2] Photocycloaddition of Atropisomeric Maleimides 1



the first step is the formation of the triplet 1,4-diradical (labeled as **DR1–DR4**), and the second step is the cyclization, in which the triplet 1,4-diradical undergoes intersystem crossing to the corresponding singlet 1,4-diradical, which recombines to form the cyclobutane photoproduct **2** or **3**. While this general mechanism is applicable to the formation of the photoproduct, the type of diradical that is preferred would dictate the *exo/endo* photoproduct selectivity (Scheme 5). To appreciate this aspect, one has to determine the carbon atoms involved in the initial bond-forming step. In the present case, the *exo* photoproduct **2** could be rationalized on the basis of the conformation “1-conf(A)” in which the terminal CH<sub>2</sub> in the alkenyl side chain is oriented away from the maleimide R<sup>1</sup> substituent, leading to diradical intermediate **DR1** or **DR2** depending on the initial bond formation between the alkene units. Similarly, formation of the *endo* photoproduct **3** could be rationalized on the basis of the conformation “1-conf(B)” in which the terminal CH<sub>2</sub> in the alkenyl side chain is oriented toward the maleimide R<sup>1</sup> substituent, leading to diradical intermediate **DR3** or **DR4** depending on the initial bond formation between the alkene units.

To understand the initial bond-forming step, we performed scrambling studies on atropisomeric maleimides **1c** and **1d** that are monosubstituted at the terminal carbon (Scheme 6). For simplicity, we will rationalize our observations for the *exo* photoproduct **2**, as one can extend similar arguments for the formation of the *endo* product **3**. For both monosubstituted maleimides, we did not observe any scrambling of the alkene geometry in the photoproduct (Scheme 6). For example, in the case of **1c** we observed the exclusive formation of **2c** as the major product, with only a trace amount of **2d**.<sup>21</sup> Scrambling studies on **1d** also displayed similar preferential formation of **2d** (Scheme 6). This could be explained by only two plausible scenarios. In the first scenario, the lack of scrambling in the

### Scheme 6. Scrambling Studies with Maleimides 1c and 1d<sup>a</sup>

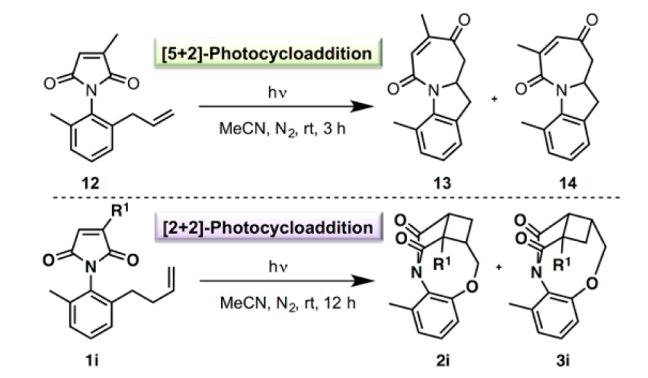


<sup>a</sup>For clarity, the *endo* photocycloadduct **3** has been omitted from the scheme.

alkene geometry indicates that during the formation of photoproduct **2** the 1,4-diradical **DR1** is likely preferred over **DR2**. In the second scenario, if indeed **DR2** is formed during the reaction, the lack of scrambling indicates that the cyclization occurs at a higher rate, so that the relative orientation of the substituents is maintained in the photoproduct in order for the reaction to maintain stereospecificity as observed. As the sensitized reaction occurs from the triplet state, the two diradicals **DR1** and **DR2** will be in the triplet manifold. For the cyclization step, this triplet 1,4-diradical has to undergo intersystem crossing to the corresponding singlet diradical so that it can recombine to form the *exo* product. Because of this spin-restricted recombination, it is likely that **DR2** is not preferred, as it would have sufficient time to scramble the alkene geometry, which would be reflected in the product distribution. In other words, the formation of the *exo* product **2** could be rationalized on the basis of the formation of **DR1** as the likely 1,4-diradical intermediate. While this is not direct evidence that conclusively rules out the formation of **DR2**, the absence of scrambling products suggests that the formation of **DR1** may be the likely pathway, as the molecular restriction will not scramble the relative orientation of the substituents on the alkenyl tether. Similar arguments may be extended to the formation of *endo* product **3**, where the preferential formation of **DR3** over **DR4** (Scheme 6) could be rationalized for the observed lack of scrambling in substrates **1c** and **1d**.

Having hypothesized the likely mechanistic rationale for triplet-sensitized irradiations, we turned our attention to direct irradiations, which gave the same selectivity in the photoproduct (ee and dr values) as the triplet-sensitized reactions, albeit with longer irradiation times. It is well-established in the literature that upon direct irradiation *N*-alkylmaleimides undergo [5 + 2] photocycloaddition from the singlet excited state.<sup>8</sup> In the case of atropisomeric maleimides **1**, direct irradiation resulted exclusively in [2 + 2] photocycloaddition. The results could be a manifestation of two different scenarios: (a) direct irradiation results in the triplet excited state as a result of fast intersystem crossing from the excited singlet state or (b) atropisomeric maleimides react from the singlet excited state to give the same photoproduct. To decipher this, we designed *o*-allyl-substituted maleimide **12** (Scheme 7), which upon photoexcitation gave [5 + 2] cycloaddition products **13** and **14** exclusively, while the corresponding butenyl analogue **1i** (with an additional CH<sub>2</sub>) as well as the *O*-allyl derivative **1a** gave the [2 + 2] photoadduct exclusively (Table 2, entries 1 and 9). This clearly indicated that the chemoselectivity in maleimides **1** is dictated by the length of the alkenyl chain at the ortho position. Additionally our photophysical studies revealed a very low intersystem crossing efficiency for the

## Scheme 7. Alkenyl Chain Length-Dependent Chemoselectivity in Atropisomeric Maleimides

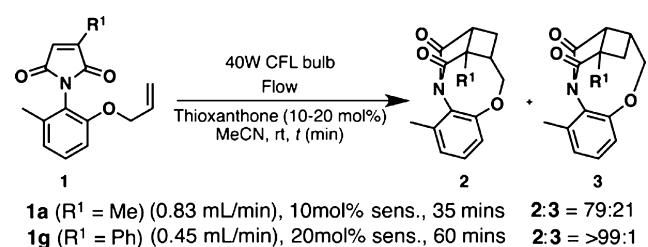


maleimides (Figure 3). These observations point to the likely involvement of a singlet excited state upon direct irradiation of the maleimides (with the maleimide chromophore absorbing light), with the reaction occurring in a concerted fashion leading to the [2 + 2] photocyclization.<sup>20</sup> The involvement of the singlet excited state upon direct irradiation is further reflected in the similar conversions observed under N<sub>2</sub>- and O<sub>2</sub>-saturated atmospheres. In addition, the involvement of the singlet excited state has literature precedent, as intramolecular photodimerization of maleimides was postulated to occur from the singlet excited state through exciplex formation.<sup>16</sup> We believe that upon direct excitation, a similar scenario is manifested in our system, leading to the photoproduct. As it involves a concerted mechanism, the bond formation is once again likely dictated by the conformational preference as well as the electron density of the interacting orbitals. As the alkene tether is electron-rich (as a result of alkyl substitution), the concerted cyclization is likely triggered by the interaction of the half-filled  $\pi$  orbital of the  $\pi\pi^*$  excited state of the maleimide with the  $\pi$  orbital of the terminal alkene.<sup>20</sup> This  $\pi(\text{maleimide}) \leftarrow \pi(\text{alkene})$  interaction is dictated by the R<sup>1</sup> substituent and is manifested in the *exo/endo* selectivity.

Thus, unlike *N*-alkenylmaleimides, which react differently from the singlet and triplet excited states leading to [5 + 2] and [2 + 2] cycloadditions, respectively,<sup>8</sup> atropisomeric maleimides with *N*-aryl substitution with an alkenyl tether at the ortho position exclusively undergo [2 + 2] photocycloaddition. We believe this chemoselectivity is a direct manifestation of molecular restraints placed on the reacting double bonds by the high barrier for N–C(aryl) bond rotation.

Our photophysical studies clearly established thioxanthone as an effective triplet sensitizer, which prompted us to evaluate visible-light irradiation conditions for [2 + 2] photocycloaddition of maleimides (Scheme 8). Such an attempt seemed very

## Scheme 8. Visible-Light Photocatalysis of Atropisomeric Maleimides 1a and 1g under Flow Conditions



appealing, as the reaction would be redox-neutral and metal-free. We were also successful in merging visible-light photolysis<sup>22</sup> with a flow setup, as it increased the efficiency and scalability of the photoreaction relative to conventional batch mode.<sup>10b,23</sup> With the simplest setup available at our disposal, we built a custom flow setup, optimized the conditions, and subjected maleimides 1a and 1g to visible-light photoreaction using a 40 W compact fluorescent lamp (CFL) as the light source.<sup>12</sup> Complete conversion of maleimide 1a was achieved (3.9 mM with 10 mol % sensitizer and a flow rate of 0.83 mL/min) within 35 min of irradiation, while the batch mode for the similar scale gave 23% conversion in 35 min. Similarly, complete conversion of 1g was achieved (1.9 mM with 20 mol % sensitizer and a flow rate of 0.45 mL/min) in less than 60 min (18% conversion for batch mode). These results clearly illustrated the efficiency of [2 + 2] photo-reactions of maleimides even under visible-light conditions.

## CONCLUSION

Our present study demonstrates the efficient stereospecific [2 + 2] photocycloaddition of atropisomeric maleimides with excellent stereocontrol in the photoproduct. The axial chirality was efficiently transferred during [2 + 2] photocycloaddition, leading to very high enantioselectivity in the photoproducts. On the other hand, the diastereoselectivity in the photoproducts is dictated by the substituents on the double bonds. Substitution at the maleimide double bond exerts a greater influence over the diastereoselectivity (*exo/endo*) than substitution on the alkenyl tether. The photoreactivity can be efficiently scaled up using visible-light mediated metal-free photocatalytic conditions under flow without any loss of selectivity in the photoproducts compared with batch-mode irradiations. As maleimides are potential targets for the construction of useful synthetic blocks (e.g., indolines), our study opens up the possibility to build complex molecular architectures with these systems with excellent stereocontrol.

## ASSOCIATED CONTENT

## Supporting Information

Experimental procedures, single-crystal XRD data (CIF), characterization data, analytical conditions, flow setup, and photophysical studies. This material is available free of charge via the Internet at <http://pubs.acs.org>.

## AUTHOR INFORMATION

## Corresponding Author

sivaguru.jayaraman@ndsu.edu

## Author Contributions

<sup>§</sup>E.K. and R.R. contributed equally.

## Notes

The authors declare no competing financial interest.

## ACKNOWLEDGMENTS

The authors from NDSU thank NSF for generous support (CHE-1213880). E.K. and J.S. thank the NSF ND-EPSCoR for a doctoral dissertation fellowship (EPS-0814442). S.J. thanks NSF for support (CHE-1111392). The authors also thank NSF-CRIF (CHE-0946990) for the purchase of the departmental X-ray diffractometer. This manuscript is dedicated to Dr. D. K. Srivastava, Professor of Chemistry and Biochemistry, North Dakota State University, an esteemed colleague and friend on the occasion of his 60th birthday.

## REFERENCES

- (1) Cahn, R. S.; Ingold, C.; Prelog, V. *Angew. Chem., Int. Ed. Engl.* **1966**, *5*, 385–415.
- (2) (a) Rau, H. *Chem. Rev.* **1983**, *83*, 535–547. (b) Inoue, Y. *Chem. Rev.* **1992**, *92*, 741–770. (c) Inoue, Y. In *Chiral Photochemistry*; Inoue, Y., Ramamurthy, V., Eds.; Molecular and Supramolecular Photochemistry, Vol. 11; Marcel Dekker: New York, 2004; pp 129–177.
- (3) (a) Bos, P. H.; Antalek, M. T.; Porco, J. A., Jr.; Stephenson, C. R. *J. Am. Chem. Soc.* **2013**, *135*, 17978–17982. (b) Kumar, N. N. B.; Mukhina, O. A.; Kutateladze, A. G. *J. Am. Chem. Soc.* **2013**, *135*, 9608–9611. (c) Maskill, K. G.; Knowles, J. P.; Elliott, L. D.; Alder, R. W.; Booker-Milburn, K. I. *Angew. Chem., Int. Ed.* **2013**, *52*, 1499–1502.
- (4) (a) Ramamurthy, V. *Photochemistry in Organized and Constrained Media*; Wiley-VCH: New York, 1991; pp 429–493. (b) Gamlin, J. N.; Jones, R.; Leibovitch, M.; Patrick, B.; Scheffer, J. R.; Trotter, J. *Acc. Chem. Res.* **1996**, *29*, 203–209. (c) Bach, T.; Bergmann, H.; Grosch, B.; Harms, K. *J. Am. Chem. Soc.* **2002**, *124*, 7982–7990. (d) Garcia-Garibay, M. A. *Acc. Chem. Res.* **2003**, *36*, 491–498. (e) Sivaguru, J.; Natarajan, A.; Kaanumalle, L. S.; Shailaja, J.; Uppili, S.; Joy, A.; Ramamurthy, V. *Acc. Chem. Res.* **2003**, *36*, 509–521. (f) Mori, T.; Weiss, R. G.; Inoue, Y. *J. Am. Chem. Soc.* **2004**, *126*, 8961–8975. (g) Veerman, M.; Resendiz, M. J. E.; Garcia-Garibay, M. A. *Org. Lett.* **2006**, *8*, 2615–2617. (h) Yang, C.; Mori, T.; Origane, Y.; Ko, Y. H.; Selvapalam, N.; Kim, K.; Inoue, Y. *J. Am. Chem. Soc.* **2008**, *130*, 8574–8575. (i) Vallavoju, N.; Selvakumar, S.; Jockusch, S.; Sibi, M. P.; Sivaguru, J. *Angew. Chem., Int. Ed.* **2014**, *126*, 5710–5714.
- (5) (a) Clayden, J. *Angew. Chem., Int. Ed. Engl.* **1997**, *36*, 949–951. (b) Ates, A.; Curran, D. P. *J. Am. Chem. Soc.* **2001**, *123*, 5130–5131. (c) Clayden, J. *Chem. Commun.* **2004**, 127–135. (d) Campolo, D.; Gastaldi, S.; Roussel, C.; Bertrand, M. P.; Nechab, M. *Chem. Soc. Rev.* **2013**, *42*, 8434–8466. (e) Honda, A.; Waltz, K. M.; Carroll, P. J.; Walsh, P. J. *Chirality* **2003**, *15*, 615–621.
- (6) (a) Ayitou, A. J.-L.; Sivaguru, J. *J. Am. Chem. Soc.* **2009**, *131*, 5036–5037. (b) Ayitou, A. J.-L.; Clay, A.; Kumarasamy, E.; Jockusch, S.; Sivaguru, J. *Photochem. Photobiol. Sci.* **2014**, *13*, 141. (c) Kumarasamy, E.; Jesuraj, J. L.; Omlid, J. N.; Ugrinov, A.; Sivaguru, J. *J. Am. Chem. Soc.* **2011**, *133*, 17106–17109. (d) Ayitou, A. J.-L.; Fukuhara, G.; Kumarasamy, E.; Inoue, Y.; Sivaguru, J. *Chem.—Eur. J.* **2013**, *19*, 4327–4334. (e) Kumarasamy, E.; Sivaguru, J. *Chem. Commun.* **2013**, *49*, 4346–4348. (f) Ayitou, A. J.-L.; Jesuraj, J. L.; Barooah, N.; Ugrinov, A.; Sivaguru, J. *J. Am. Chem. Soc.* **2009**, *131*, 11314–11315. (g) Jesuraj, J. L.; Sivaguru, J. *Chem. Commun.* **2010**, *46*, 4791–4793. (h) Raghunathan, R.; Kumarasamy, E.; Iyer, A.; Ugrinov, A.; Sivaguru, J. *Chem. Commun.* **2013**, *49*, 8713–8715.
- (7) (a) Obata, T.; Shimo, T.; Suishu, T.; Somekawa, K. *J. Heterocycl. Chem.* **1998**, *35*, 1361–1364. (b) Booker-Milburn, K. I.; Anson, C. E.; Clissold, C.; Costin, N. J.; Dainty, R. F.; Murray, M.; Patel, D.; Sharpe, A. *Eur. J. Org. Chem.* **2001**, 1473–1482. (c) Tedaldi, L. M.; Aliev, A. E.; Baker, J. R. *Chem. Commun.* **2012**, *48*, 4725–4727. (d) Bradshaw, J. S. *Tetrahedron Lett.* **1966**, *7*, 2039–2042.
- (8) Roscini, C.; Cubbage, K. L.; Berry, M.; Orr-Ewing, A. J.; Booker-Milburn, K. I. *Angew. Chem., Int. Ed.* **2009**, *48*, 8716–8720.
- (9) Cubbage, K. L.; Orr-Ewing, A. J.; Booker-Milburn, K. I. *Angew. Chem., Int. Ed.* **2009**, *48*, 2514–2517.
- (10) (a) Hook, B. D. A.; Dohle, W.; Hirst, P. R.; Pickworth, M.; Berry, M. B.; Booker-Milburn, K. I. *J. Org. Chem.* **2005**, *70*, 7558–7564. (b) Knowles, J. P.; Elliott, L. D.; Booker-Milburn, K. I. *Beilstein J. Org. Chem.* **2012**, *8*, 2025–2052.
- (11) (a) Kitagawa, O.; Izawa, H.; Sato, K.; Dobashi, A.; Taguchi, T.; Shiro, M. *J. Org. Chem.* **1998**, *63*, 2634–2640. (b) Duan, W.-L.; Imazaki, Y.; Shintani, R.; Hayashi, T. *Tetrahedron* **2007**, *63*, 8529–8536.
- (12) See the Supporting Information.
- (13) Miller, C. W.; Jönsson, E. S.; Hoyle, C. E.; Viswanathan, K.; Valente, E. J. *J. Phys. Chem. B* **2001**, *105*, 2707–2717.
- (14) (a) Shimizu, K. D.; Freyer, H. O.; Adams, R. D. *Tetrahedron Lett.* **2000**, *41*, 5431–5434. (b) Bennett, D. J.; Pickering, P. L.; Simpkins, N. S. *Chem. Commun.* **2004**, 1392–1393.
- (15) HRMS analysis of the crude photolysate showed mass peaks corresponding to addition products of acetone to phenylmaleimide **1g**.
- (16) Put, J.; De Schryver, F. C. *J. Am. Chem. Soc.* **1973**, *95*, 137–145.
- (17) Gülten, Ş.; Sharpe, A.; Baker, J. R.; Booker-Milburn, K. I. *Tetrahedron* **2007**, *63*, 3659–3671.
- (18) Dalton, J. C.; Montgomery, F. C. *J. Am. Chem. Soc.* **1974**, *96*, 6230–6232.
- (19) Schmidt, R.; Tanielian, C.; Dunsbach, R.; Wolff, C. *J. Photochem. Photobiol., A* **1994**, *79*, 11–17.
- (20) Turro, N. J.; Ramamurthy, V.; Scaiano, J. C. *Modern Molecular Photochemistry of Organic Molecules*; University Science Books: Sausalito, CA, 2010; pp 705–799.
- (21) Similar results were obtained by photoreaction of **1c** performed with thioxanthone sensitization using 420 nm irradiation in a Rayonet reactor.
- (22) (a) Yoon, T. P.; Ischay, M. A.; Du, J. *Nat. Chem.* **2010**, *2*, 527–532. (b) Narayanam, J. M. R.; Stephenson, C. R. *J. Chem. Soc. Rev.* **2011**, *40*, 102–113. (c) Ismaili, H.; Pitre, S. P.; Scaiano, J. C. *Catal. Sci. Technol.* **2013**, *3*, 935–937. (d) Schultz, D. M.; Yoon, T. P. *Science* **2014**, *343*, No. 1239176. (e) Alonso, R.; Bach, T. *Angew. Chem., Int. Ed.* **2014**, *53*, 4368–4371.
- (23) Tucker, J. W.; Zhang, Y.; Jamison, T. F.; Stephenson, C. R. *J. Angew. Chem., Int. Ed.* **2012**, *51*, 4144–4147.